Molecular junctions

DOI: 10.1002/smll.200700287

Modulating the Conductance of a Au–octanedithiol–Au Molecular Junction**

*Bingqian Xu**

Electron transport through a single molecule is a central theme in molecular electronics. The ability to measure the conductance of a single molecule not only offers a new way to approach many interesting and fundamental problems in nanometer-scale science, but is also a necessary step towards the goal of building devices using single molecules. In order to measure single-molecule conductance, a molecular junction with a single molecule wired up to probe electrodes has to be fabricated. It is also essential to be able to efficiently and precisely control electron transport through such molecular junctions and understand the details of the factors that affect the transport before such devices can be made practical. Methods for connecting molecules mainly include mechanically controlled break junctions,[1,2] scanning tunneling microscopy (STM),[3,4] conducting atomic force microscopy,[5,6] nanopores,[7,8] crossed wires,[9] mercury drop contacts,[10] electrostatic trapping,[11] bridging two closely spaced SAM-functionalized electrode surfaces with a metallic nanoparticle,[12,13] and self-assembled monolayers.[14] Each method has some particular advantages[8] but the difficulty of counting the number of contacted molecules, and the characterization of their bonding, are still challenging problems.

Although the molecule consists of a series of discrete states in a small, finite entity, the electrodes contain a very dense set of continuous states in a macroscopic structure. When a molecule is sandwiched between electrodes to form a molecular junction, electron transport is not only determined by the molecule itself but also influenced by molecule–electrode contacts, and the latter can sometimes dominate electron transport. Unfortunately, the nature of the electrode–molecule contacts and the specific geometry have been the least controllable aspects of the experiments that ultimately determines the measured current and thus need a systematic investigation. Theoretical calculations using density functional theory and first-principles analysis show that both the bonding force and the conductance are sensitive to distance between the molecule and the contact, extra metal atoms at the Au surface, binding sites, molecular orientation, and bias voltage.[15–17] A reliable method for measuring the conductance of a molecule must provide a reproducible electronic coupling between the molecule and probing electrodes.[6,18–20] In order to make comparison with theory, single molecules or at least a countable number of molecules have to be connected with the electrodes. Tao and coworkers developed the STM break-junction method and used it to study various issues in single-molecule conductance, including the molecule–electrode contacts,[21–23] and generated some agreements with theoretical studies; it is a promising method due to its simplicity. However, a detailed study of the role of contact geometry in molecular junctions is still one of the least touched-upon issues and needs further investigation.[24]

This Communication reports a study focusing on molecule–electrode contact effects on the conductance of a single octanedithiol (C_8) molecule by combining an STM break-junction method[25] with STM piezoelectric transducer (PZT) modulation. In order to do this, an ac signal was applied to the STM PZT to *regularly* modulate the contact configurations by varying the distance between the substrate and tip. The conductance fluctuations of the molecular junctions were monitored simultaneously (Figure 1). A C_8-based molecule was chosen as the test molecule for this study for the following reasons: First, the molecule is terminated with thiol groups on both ends so that they can covalently bind to two Au electrodes simultaneously. Secondly, it has a rather large HOMO–LUMO gap and its conduction mechanism is due to electron tunneling.[5,10,25–28] Generally, conductance of a molecular junction results from electron injection into the molecule combined with the intrinsic conductance of the molecule. At low bias voltage, the chemical potentials of the electrodes are far from the HOMO and LUMO energy levels of the molecule and thus the main contribution to the conductance comes from the metal electrode–molecule junction potential mismatch, which can be changed using PZT modulations. Finally, this molecule has been widely studied by various techniques.[5,10,25–29]

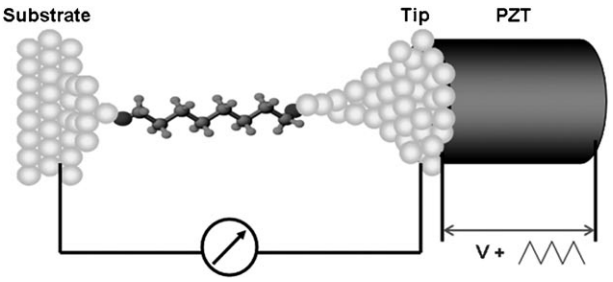

Figure 1. Schematic illustration of a single-molecule conductance measurement with contact configuration modulations. The experiment was carried out by superimposing a small ac voltage to the piezoelectric transducer (PZT) while repeatedly stretching the molecular junction using the STM break-junction method.

We first measured the conductance of the single C_8 molecule in toluene without PZT modulations. About 40% of the transient conductance curves have clear conductance plateaus (Figure 2a) and were used to construct the conduc-

[*] Prof. Dr. B. Xu
Molecular Nanoelectronics
Faculty of Engineering & Nanoscale Science and Engineering Center
University of Georgia, Athens, GA 30602 (USA)
Fax: (+1) 706-542-8806
E-mail: bxu@engr.uga.edu

[**] University of Georgia start-up grants and UGARF faculty research fund are acknowledged for financial support.

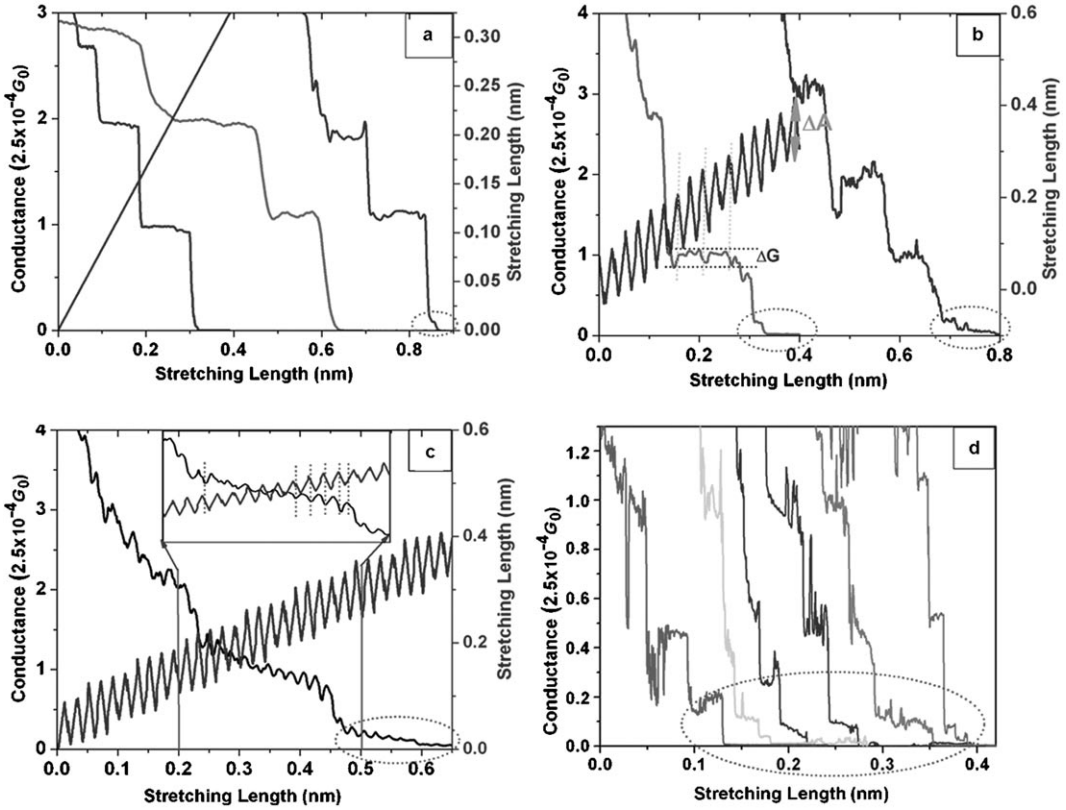

Figure 2. a) Transient conductance curves of a 1,8-octanedithiol molecule covalently bonded to two gold electrodes. The measurements were performed in toluene containing 1 mM octanedithiol without PZT modulation. The major conductance plateaus are mostly around the integer multiples of $2.5 \times 10^{-4} G_0$ with very small fluctuations. b) Typical curves obtained with PZT modulations, with a modulation amplitude (ΔA) of 1 Å and a frequency of 500 Hz. The conductance fluctuates (ΔG) around the major conductance value of $2.5 \times 10^{-4} G_0$ with a phase shift of about 180°. c) A conductance curve showing a more pronounced 180° phase shift between the PZT modulation and the conductance fluctuation. d) The magnified conductance curves show conductance plateaus below the major $2.5 \times 10^{-4} G_0$ step under PZT modulation.

tance histogram. The remaining 60% of the curves were excluded when constructing conductance histograms because some of them are too noisy to identify plateaus and the others decay exponentially and lack clear plateaus. The histogram (the bar graph in Figure 3) reveals two sets of peaks. The major peaks are located at integer multiples of $2.5 \times 10^{-4} G_0$, with additional minor peaks located at conductance values about one quarter of $2.5 \times 10^{-4} G_0$, which agrees well with earlier experimental results.[21,22,25,30] However, the heights of the major peaks are much larger than those of the minor peaks. These peaks have been attributed to the two S–Au contact configurations, namely, top contact and hollow contact,[22] reflecting complex contact geometry disorder during the junction stretching process. Such geometric disorder can strongly affect charge transport through these junctions and give rise to the random switching phenomena often seen experimentally in such structures. In addition, both experimental and theoretical studies suggested that Au–Au bonds break when breaking the Au–octanedithiol–Au molecular junctions.[21] Therefore, electrode geometry changes due to Au-atom motion add to the complexity of the system.

In order to study the effects of extra complexity resulting from the geometric disorder inherent in metal–molecule bonding on the single-molecule conductance, ac signals with

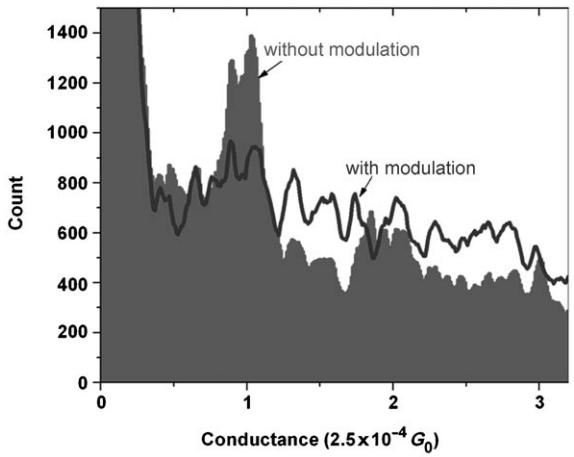

Figure 3. Conductance histograms of C_8 molecular junctions with (line graph) and without (bar graph) PZT modulations. Two sets of conductance peaks located at multiple integers of $2.5 \times 10^{-4} G_0$ (major peaks) and of $5 \times 10^{-5} G_0$ (minor peaks) are observed in both cases, but with different heights; the major conductance peaks are much higher than the minor ones without PZT modulations (bar graph) but these height differences diminish when PZT modulations are applied (line graph).

a frequency of 500 Hz and different amplitudes were applied over the STM PZT and measurements of the Au–octanedithiol–Au molecular junctions were repeated. 500 Hz modulation is very slow compared with the intermolecular conformational motion and thus the molecule has sufficient time to adapt to the instantaneous local geometry. Three evident and repeatable effects were observed.

First, the conductance of the molecular junction containing a single C_8 molecule fluctuates around $2.5\times10^{-4}G_0$. Figure 2a shows three transient conductance curves obtained without applying the PZT modulation. The single-molecule conductance was determined to be $\approx2.5\times10^{-4}G_0$ (shown as the last major plateau in the conductance curves). The plateaus in the curves were rather flat. In addition to these major plateaus, some of the conductance curves also have minor plateaus with a conductance of one quarter of $2.5\times10^{-4}G_0$ (not shown in Figure 2a). Figure 2b–d shows examples of transient conductance curves under PZT modulation. It was found that single-molecule conductance fluctuates rather regularly with a fluctuation amplitude ΔG at the last plateau (Figure 2b), but has a phase shift of about 180° in relation to the PZT modulation (Figure 2b and c). This result is reasonably understandable because a longer molecular junction should hava a smaller conductance. But whether it has an exponential dependence is not certain at this stage.

Second, although conductance fluctuation (ΔG) of different individual conductance curves varies from curve to curve with the same PZT modulation, the averaged relative conductance fluctuation ($\Delta G/G$) changes rather regularly under different PZT modulation. In a series of experiments, $\Delta G/G$ under different PZT modulation amplitudes (ΔA) at a fixed frequency (500 Hz) was investigated (Figure 4a). The frequency was chosen such that there are at least three circles on the last plateau of the conductance curves. It was found that $\Delta G/G$ differs from each individual conductance curves; this possibly indicates the initial microscopic details of each of the molecular junction, over which there is no control. In order to see the overall effect of averaged behavior of many such junctions, the $\Delta G/G$ histogram (insert of Figure 4a) was used to determine the most probable values of $\Delta G/G$ of the single molecule (at the last plateau of the conductance curve). $\Delta G/G$ increases with ΔA tremendously when ΔA increases from 0.2–0.4 Å, and then with a slow increase with ΔA from 0.4–0.8 Å. Upon further increasing ΔA, $\Delta G/G$ seems to reach a maximum value at ≈0.23 (Figure 4a). When ΔA is over 1.2 Å, the conductance curves become so noisy that it is not possible to recognize any clear plateaus in the conductance curves, which suggests that the perturbation is too large to form a molecular junction. Surprisingly, by measuring the stretching length (the distance over which a molecular junction can be stretched before breaking, L, as shown in Figure 2b) of each single-molecule junction and determining the most probable value for L using the histogram, we found that L increases with ΔA until $\Delta A\approx1$ Å, then decreases rapidly (Figure 4b). This could be explained by the PZT modulation dramatically increasing the local temperature of the junction and producing Au–Au bond breakage, which may have the same origin as current-induced local heating effects in molecular junctions.

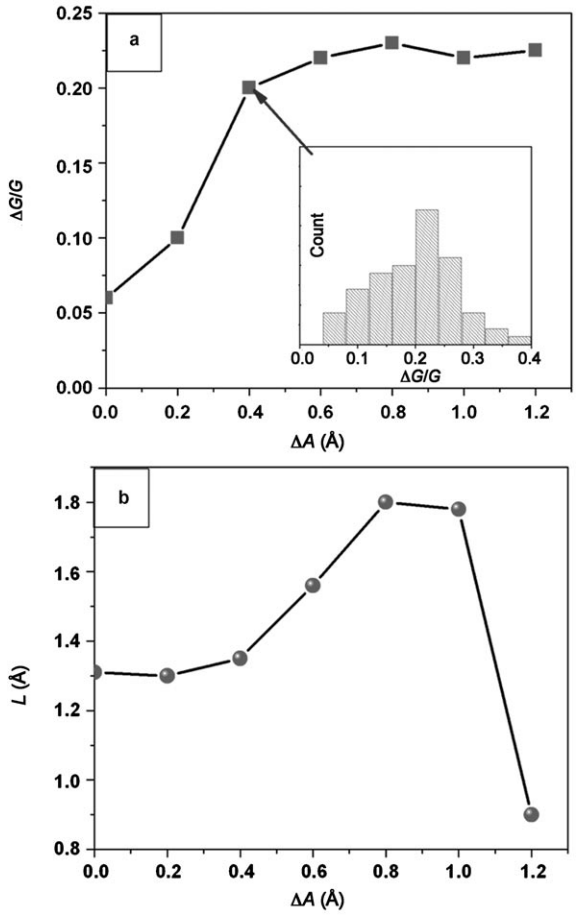

Figure 4. a) The relative single C_8-molecule conductance fluctuation amplitude ($\Delta G/G$) versus PZT modulation amplitude (ΔA). The value of $\Delta G/G$ used in the plot was determined using peak values in the $\Delta G/G$ histograms (see inset). b) The stretching length (L) of the single C_8-molecular junction versus PZT modulation amplitude.

Lastly, in addition to causing pronounced conductance fluctuations around the major conductance steps, PZT modulations also generate much greater numbers of smaller conductance plateaus below the major $2.5\times10^{-4}G_0$ plateau. Figure 2d shows some typical conductance curves that have such smaller conductance plateaus recorded during the PZT modulation. Although conductance plateaus can appear at any smaller conductance values (indicating the microscopic details of molecule electrode contact), the peak values in the conductance histogram (line plot in Figure 3) suggest that the molecule–electrode contacts have some most-probable configurations with a conductance four times smaller than the main value of $2.5\times10^{-4}G_0$. However, multiple small plateaus can appear together with the major plateau (Figure 2d), strongly suggesting more-complex contact geometries due to small structure changes at the molecule-electrode contacts caused by the PZT modulations. These changes, in this case, can include distance changes between the molecule and the contact and contact geometry changes. It was also noticed that the most frequently observed con-

ductance plateau is that with a conductance of only $\approx 1/10$ of the value of the main plateau (as highlighted with dotted ovals in Figure 2). This plateau suggests that no matter what contact geometry the junction originally is, the molecule–contact configuration just before breaking of the molecular junction is always the same.

The averaged single-molecule conductance was compared by constructing conductance histograms from ≈ 800 individual measurements in both cases. As shown in Figure 3, the conductance of the C_8 molecular junction can be any value because of the sensitive dependence of the conductance on the microscopic details of the molecule–electrode contacts. Without PZT modulation, the histogram (bar graph in Figure 3) reveals well-defined major peaks at integer multiples of a fundamental conductance value ($2.5 \times 10^{-4} G_0$), which is used as the signature to identify the conductance of the single C_8 molecular junction without PZT modulation. Less-pronounced peaks at one quarter of the major conductance were also found to be superimposed on the histogram. When a PZT modulation with an amplitude of 1 Å and a frequency of 500 Hz was applied, however, the peaks in the conductance histogram become almost equally pronounced with similar probability. This can be explained by considering that extra contact configurations with different conductance were generated under the PZT modulations, and thus the probability of obtaining the major conductance plateaus was reduced.

In summary, molecule–electrode contact effects were studied on a single C_8-based molecule covalently connected to two gold electrodes to form a repeatedly created gold–molecule–gold junction using a technique that combines STM break-junction methods with PZT modulation. The conductance histogram constructed from the repeated measurements with and without the PZT modulation reveal two sets of well-defined peaks at integer multiples of two fundamental conductance values. The lower ones occur much more frequently with the PZT modulation and have a conductance that is ≈ 4 times smaller. The averaged relative conductance fluctuation ($\Delta G/G$) changes regularly under different PZT modulation and can be as large as $\Delta G/G \approx 0.23$ at about $2.5 \times 10^{-4} G_0$. The maximum perturbation amplitude that a molecular junction with thiol–gold contacts can suffer is ≈ 1 Å. The change in conductance of the single C_8 molecular junction under PZT modulation is due to the change of distance between the molecule and the contact, extra metal atoms at the Au surface, binding sites, and molecular orientation. In order to better understand the contact issues in molecular junctions, more experimental as well as theoretical efforts have to be made. Experiments on different combinations of contact metals and molecule linkers are under way.

Experimental Section

The SPM break-junction setup was a modified PicoPlus-SPM (Agilent-Molecular Imaging) system, interfaced with National Instruments electronics.

The Au STM tip was prepared by cutting a 0.25 mm gold wire (99.999%). The Teflon STM cell was cleaned with piranha solution and then sonicated in 18 MΩ water three times. The Au substrate was prepared by evaporating 20 nm Cr and then 150 nm Au on mica in a UHV chamber. Prior to each experiment, the substrate was briefly annealed in a hydrogen flame for 1–2 min and experiments were carried out in toluene containing 1 mM octanedithiol.

The first step was to bring the STM tip to within the tunneling distance of the substrate using the STM controller. The STM feedback was then turned off and a separate homemade Labview computer program was used to move the tip into and out of contact with the substrate at a typical rate of 20–40 nm s^{-1} by generating a triangular voltage wave function over the PZT. At the same time a small ac signal was superimposed on the PZT (Figure 1). The transient conductance curves during the process were recorded with a digital oscilloscope.

Keywords:
conductance · gold · molecular electronics · molecular junctions · scanning probe microscopy

[1] A. Salomon, D. Cahen, S. Lindsay, J. Tomfohr, V. B. Engelkes, C. D. Frisbie, *Adv. Mater.* **2003**, *15*, 1881–1890.
[2] S. N. Yaliraki, M. Kemp, M. A. Ratner, *J. Am. Chem. Soc.* **1999**, *121*, 3428–3434.
[3] F. Moresco, L. Gross, M. Alemani, K. H. Rieder, H. Tang, A. Gourdon, C. Joachim, *Phys. Rev. Lett.* **2003**, *91*, 036601-1–036601-4.
[4] M. Magoga, C. Joachim, *Phys. Rev. B* **1997**, *56*, 4722–4729.
[5] X. D. Cui, A. Primak, X. Zarate, J. Tomfohr, O. F. Sankey, A. L. Moore, T. A. Moore, D. Gust, G. Harris, S. M. Lindsay, *Science* **2001**, *294*, 571–574.
[6] M. A. Reed, C. Zhou, C. J. Muller, T. P. Burgin, J. M. Tour, *Science* **1997**, *278*, 252–254.
[7] M. Mayor, C. von Hanisch, H. B. Weber, J. Reichert, D. Beckmann, *Angew. Chem. Int. Ed.* **2002**, *41*, 1183–1186.
[8] L. A. Bumm, J. J. Arnold, M. T. Cygan, T. D. Dunbar, T. P. Burgin, L. Jones, D. L. Allara, J. M. Tour, P. S. Weiss, *Science* **1996**, *271*, 1705–1707.
[9] A. S. Blum, J. G. Kushmerick, S. K. Pollack, J. C. Yang, M. Moore, J. Naciri, R. Shashidhar, B. R. Ratna, *J. Phys. Chem. B* **2004**, *108*, 18124–18128.
[10] D. J. Wold, C. D. Frisbie, *J. Am. Chem. Soc.* **2001**, *123*, 5549–5556.
[11] C. Zhou, M. R. Deshpande, M. A. Reed, L. Jones, J. M. Tour, *Appl. Phys. Lett.* **1997**, *71*, 611–613.
[12] J. Chen, M. A. Reed, A. M. Rawlett, J. M. Tour, *Science* **1999**, *286*, 1550–1552.
[13] J. G. Kushmerick, D. B. Holt, S. K. Pollack, M. A. Ratner, J. C. Yang, T. L. Schull, J. Naciri, M. H. Moore, R. Shashidhar, *J. Am. Chem. Soc.* **2002**, *124*, 10654–10655.
[14] R. E. Holmlin, R. Haag, M. L. Chabinyc, R. F. Ismagilov, A. E. Cohen, A. Terfort, M. A. Rampi, G. M. Whitesides, *J. Am. Chem. Soc.* **2001**, *123*, 5075–5085.
[15] A. Bezryadin, C. Dekker, G. Schmid, *Appl. Phys. Lett.* **1997**, *71*, 1273–1275.
[16] D. P. Long, C. H. Patterson, M. H. Moore, D. S. Seferos, G. C. Bazan, J. G. Kushmerick, *Appl. Phys. Lett.* **2005**, *86*, 153105-1–153105-3.

[17] I. Amlani, A. M. Rawlett, L. A. Nagahara, R. K. Tsui, *Appl. Phys. Lett.* **2002**, *80*, 2761–2763.
[18] J. C. Love, L. A. Estroff, J. K. Kriebel, R. G. Nuzzo, G. M. Whitesides, *Chem. Rev.* **2005**, *105*, 1103–1169.
[19] A. Nitzan, M. A. Ratner, *Science* **2003**, *300*, 1384–1389.
[20] S. M. Lindsay, M. A. Ratner, *Adv. Mater.* **2007**, *19*, 23–31.
[21] R. L. York, P. T. Nguyen, K. Slowinski, *J. Am. Chem. Soc.* **2003**, *125*, 5948–5953.
[22] B. Q. Xu, N. J. Tao, *Science* **2003**, *301*, 1221–1223.
[23] X. D. Cui, A. Primak, X. Zarate, J. Tomfohr, O. F. Sankey, A. L. Moore, T. A. Moore, D. Gust, L. A. Nagahara, S. M. Lindsay, *J. Phys. Chem. B* **2002**, *106*, 8609–8614.
[24] C. E. D. Chidsey, *Science* **1991**, *251*, 919–922.
[25] W. Y. Wang, T. Lee, M. A. Reed, *Phys. Rev. B* **2003**, *68*, 036601-1–036601–4.
[26] B. Q. Xu, X. L. Li, X. Y. Xiao, H. Sakaguchi, N. J. Tao, *Nano Lett.* **2005**, *5*, 1491–1495.
[27] X. L. Li, J. He, J. Hihath, B. Q. Xu, S. M. Lindsay, N. J. Tao, *J. Am. Chem. Soc.* **2006**, *128*, 2135–2141.
[28] X. Y. Xiao, B. Q. Xu, N. J. Tao, *Nano Lett.* **2004**, *4*, 267–271.
[29] M. Mayor, H. B. Weber, *Angew. Chem.* **2004**, *116*, 2942–2944; *Angew. Chem. Int. Ed.* **2004**, *43*, 2882–2884.
[30] Y. B. Hu, Y. Zhu, H. J. Gao, H. Guo, *Phys. Rev. Lett.* **2005**, *95*, 156803-1–156803-4.

Received: April 24, 2007
Revised: September 26, 2007
Published online on November 19, 2007

